Heliyon 6 (2020) e05413

Contents lists available at ScienceDirect

Heliyon

journal homepage: www.cell.com/heliyon

Research article

Photo-assisted bio-fabrication of silver nanoparticles using *Annona muricata* leaf extract: exploring the antioxidant, anti-diabetic, antimicrobial, and cytotoxic activities

J.A. Badmus [a,c,*], S.A. Oyemomi [a], O.T. Adedosu [a], T.A. Yekeen [b], M.A. Azeez [b], E.A. Adebayo [b], A. Lateef [b], U.M. Badeggi [d], S. Botha [e], A.A. Hussein [d], J.L. Marnewick [c]

[a] *Department of Biochemistry, Ladoke Akintola University of Technology, Ogbomoso, Nigeria*
[b] *Department of Pure and Applied Biology, Ladoke Akintola University of Technology, Ogbomoso, Nigeria*
[c] *Applied Microbial and Health Biotechnology Institute, Cape Peninsula University of Technology, Cape Town, South Africa*
[d] *Department of Chemistry, Cape Peninsula University of Technology, Cape Town, South Africa*
[e] *Electron Microscope Unit, University of the Western Cape, Cape Town, South Africa*

ARTICLE INFO

Keywords:
Materials science
Nanotechnology
Green synthesis
Biomedical applications
Silver nanoparticle
Annona muricata
Antioxidant
Anti-diabetic
Antimicrobial
Lipid peroxidation
Cytotoxicity

ABSTRACT

Green synthesis of metal nanoparticles is reputed to have a robust range of biomedical applications. Silver nanoparticles (AgNPs) bio-fabricated using aqueous leaf extract of *Annona muricata* were characterized and evaluated for *in-vitro* antioxidant, lipid peroxidation inhibition, anti-diabetic and antimicrobial activities as well as cytotoxicity in human keratinocyte cells (HaCaT).

The extract induced colour change of silver salt solution which absorbed at 420 nm and confirmed the formation of AgNPs. FTIR showed that free amide and hydroxyl groups were responsible for the synthesized nanoparticles. Both XRD and SAED confirmed the crystalline nature of the particles with face centered cubic (FCC) phase. The zeta potential revealed -27.2 mV potential and average distribution size of 35 nm. DLS indicated that the majority of the particles were 86.78 nm size and with a polydispersity index (PDI) of 0.329.

AgNPs displayed strong activities against DPPH (IC_{50} = 51.80 μg/ml), ABTS (IC_{50} = 30.78 μg/ml), α-amylase (IC_{50} = 0.90 μg/ml) and α-glucosidase (IC_{50} = 3.32 μg/ml). The particles exhibited a dose-dependent inhibition of Fe^{2+}-induced lipid peroxidation with effective antimicrobial activity against a battery of bacterial strains and cytotoxicity in HaCaT cell line. These findings revealed the potential biomedical applications of the particles and further work will be required to establish its molecular mechanism of action.

1. Introduction

The biological method of nanoparticle synthesis using plant extracts is considered as eco-friendly and an excellent alternative for chemical and physical methods [1]. While chemical and physical methods require high energy and chemicals for the synthesis of nanoparticles, biological agents make use of naturally occurring phytochemicals, proteins, and enzymes for the formation and possible capping of the nanohybrids [2]. Synthesis of silver nanoparticles (AgNPs) using a biological method is simple, reliable, nontoxic, and eco-friendly [3]. Green synthesized AgNPs are biocompatible and safe for several therapeutic applications. The broad biological activities of AgNPs led to its inclusion in household products such as antimicrobial agents, textiles, wound dressing agents, and antiseptic spray, to name a few [4].

The usefulness of the AgNPs found in drug delivery, diagnosis, and extensively in disease treatment has led to a positive and unprecedented growth in its study in the scientific sphere [1]. It has been found beneficial as antibacterial, anti-diabetic, antioxidative and anti-proliferative agents [5]. The plant biogenic-induced synthesis of nanoparticles is considered essential due to its anti-cancer capability and lesser side effects and various other numerous positive effects in certain diseased states [6]. Previous studies have related the anti-cancer properties of AgNPs to be via the induction of oxidative stress and mitochondria and DNA damage ultimately leading to apoptosis [7]. A number of com-

* Corresponding author.
E-mail address: jabadmus@lautech.edu.ng (J.A. Badmus).

https://doi.org/10.1016/j.heliyon.2020.e05413
Received 9 August 2020; Received in revised form 3 September 2020; Accepted 29 October 2020

pounds isolated from plants are known to be effective against diverse human ailments. Leaf extracts of plants such as *Catharanthus roseus*, *Rosmarinus officinalis*, *Camellia sinensis*, *Lantana camara* have been used to synthesize AgNPs with interesting potential biomedical applications [8, 9, 10, 11].

Annona muricata belongs to the family of Annonaceae found in tropical and subtropical parts of the world. It is a tree with a height reaching between 5-8 m and a diameter of 15–83 cm with an open roundish canopy consisting of large glossy dark green leaves [12]. Different parts of the plant are used as a cure for many illnesses in folklore treatment. It is reportedly used against inflammation, diabetes, hypertension and parasitic plague. The seed is used against worms and the fruits are used to treat arthritis and fever [13]. The leaves are used against hyper-glycaemia, inflammation, spasms and cancer [14]. Traditionally, juice from the fruits and infusion of leaves and branches are used as a sedative, against respiratory illness, malaria, gastrointestinal problems and liver, heart and kidney problems. The plant is rich in secondary metabolites such as saponins, alkaloids, flavonoids, terpenoids, annonaceous acetogenins, megastigmanes, cyclopeptides and essential oils [14]. These compounds inherent in this plant are known for the variety of useful biomedical applications. Previous studies have used different parts of the plant for the synthesis of AgNPs and confirmed that the plant contains phytochemicals with the ability to synthesize and cap AgNPs [15, 16].

Inspired by the important phytochemicals present in the plant coupled with probable important biomedical applications, this is the first synthesis of AgNPs from the plant leaves where no extraneous conditions like high temperature and organic solvents were used. In addition, this study report for the first time, the anti-diabetic, lipid peroxidation inhibitions and cytotoxic effect of the nanoparticles on an immortalized human keratinocyte cell line (HaCaT).

2. Materials and methods

2.1. Chemicals and plant collection

All chemicals used were of analytical grade purchased from Sigma-Merck (South Africa). Fresh leaves of *Annona muricata* were collected from Okeigbo in Ondo state, Nigeria and identified in the Herbarium Unit of the Department of Pure and Applied Biology, Herbarium Unit, Ladoke Akintola University of Technology, Ogbomoso, Nigeria.

2.2. Preparation of leaf extract

The leaves were air-dried under ambient environmental conditions where after they were pulverized, using an electric blender to obtain a fine powder. Leaf powder (6 g) was extracted in 100 ml Millipore water using a magnetic stirrer for 2 h at 40 °C. This was followed by cooling and filtering using Whatman No1 filter paper to obtain the aqueous leaf extract.

2.3. Silver nanoparticles synthesis

One milliliter of the aqueous leaf extract of *Annona muricata* was added to 40 ml of 1 mM $AgNO_3$ to synthesize silver nanoparticles with continuous shaking in the presence of light for 30 min [17]. The colour change to dark brown confirmed the formation of the silver nanoparticles. The particles were purified to separate any untreated reaction mixtures by centrifugation at 10 000 rpm for 25 min and repeated washing with deionized water.

2.4. Physicochemical characterization of AgNPs

UV-visible spectral analysis was used to monitor the bio-reduction of the Ag salt solution of the aqueous extract of *Annona muricata* leaves. The synthesis was monitored periodically by recording the absorbance spectral using a Polar Star Omega Microtitre Plate reader (BMG Labtech, Ortenberg, Germany) at the wavelength ranging from 200 to 700 nm. This was followed by subjecting the AgNPs to Fourier Transform Infrared Spectroscopy (FTIR) to determine functional groups that contributed to the synthesis at wavenumber ranging from 4000 cm^{-1} to 400 cm^{-1} using the Thermo Scientific TM Nicolet. X-ray diffraction (XRD) nature was carried on the particles to determine the crystal phase using the advanced model Bruker AXS D8, operated at a voltage of 40 kV and a current of 30 mA with Cu, Kα radiation (λ- 1.54056 Å) in a Θ-2Θ configuration with the range of 20–80°. TEM analysis was done on the TEM JEOL at 300 kV to determine the size and shape of the silver nanoparticles from the TEM micrograph. The elemental analysis of the nanoparticles was assessed using Energy Dispersive X-Ray Spectroscopy (EDS). Dynamic light scattering (DLS) of the nanoparticles was determined using a Malvern Zetasizer Nanoseries (Nano-ZS90) to study the phase behaviour of the particles.

2.5. Cell culture and maintenance

An immortallized keratinocyte cell line of adult human skin, HaCaT was purchased from ATCC, (USA) and used for the study. The cells were maintained in Dulbecco's Modified Eagles Medium (DMEM) containing 10% FBS and 1% PenStrep. The cells were kept at 37 °C under the humidified condition of 5% CO_2 in air.

2.6. Antioxidant assays

2.6.1. DPPH (2, 2-diphenyl-1-picrylhydrazl) scavenging activity

The method of Kim et al. [18] with slight modification was followed to evaluate DPPH scavenging potential of AgNPs. Different concentrations of AgNPs and Trolox (standard) at 100 µl were added to 100 µl of 0.25 mM DPPH (dissolved in methanol) in 96-well plate and incubated at room temperature for 30 min in the dark. The absorbance of the reaction was recorded at 517 nm using a UV-Visible spectrophotometer (Multiskan, Thermo Scientific, USA).

2.6.2. ABTS (2, 2′-azino-bis (3-ethylbenzothiazoline-6-sulfonic acid)) scavenging activity

This assay followed the standard method as described by Moldovan et al. [19] with slight modification. This involved the preparation of stock solutions of 7.4 mM ABTS and 2.6 mM potassium persulfate. Next, 80 µl of persulfate was added to 5 ml solution of ABTS and left in the dark for 12 h. A working solution was prepared by adding 2 ml of ABTS-persulfate solution to 20 ml distilled water. Varying concentrations of AgNPs and Trolox at 25 µl were added to 300 µl of the ABTS working solution. The reacting mixture was incubated at room temperature in the dark for 30 min and read at 734 nm using a UV-visible spectrophotometer (Multiskan, Thermo Scientific, USA). The percentage scavenging ability was calculated as stated in Eq. (1) below.

$$\text{Percentage inhibition} = \frac{A\ blank - A\ sample}{A\ blank} \times 100 \qquad \text{equation (1}$$

2.7. Inhibition of lipid peroxidation using egg yolk and S9 rat liver homogenates

Inhibitions of Fe^{2+}-induced *in vitro* lipid peroxidation in egg yolk and rat liver homogenates by AgNPs were carried out using the modified methods of Badmus et al. [20]. AgNPs (500 µl) at various concentration (350, 175, 87.5 and 43.75 µg/ml) was added to 500 µl of homogenate (egg yolk or liver) (10%; v/v). Then, 50 µl of 0.07 mM ferrous sulphate was added and the mixture was incubated at room temperature for 30 min. Briefly, thiobarbituric acid (1.5 ml) 0.8% in 1.1% SDS solution and 1.5 ml 10% acetic acid were added respectively. The mixture was mixed on a vortex and heated at 95 °C for 45 min to develop a pink colour. The mixture was allowed to cool and then centrifuged at 5000 rpm for 5 min.

The absorbance of the supernatant was read at 532 nm using distilled water as blank and the percentage inhibition was calculated using the formula as stated in Eq. (1).

2.8. In vitro anti-diabetic assay

2.8.1. α-Amylase inhibitory activity

The assay was evaluated by following the method described by Madhusudhan and Kirankumar [21] with slight modification. The reaction mixture in a 96-well plate contained 50 µl phosphate buffer (20 mM, pH = 6.9) with 6.7 mM sodium chloride, 20 µl α–amylase (2 U/ml), and 20 µl of varying concentrations of AgNPs and acarbose as standard. The mixture was pre-incubated for 20 min at 37 °C followed by the addition of 20 µl of 1% soluble starch as substrate (20 mM phosphate buffer pH 6.9) with a further incubation for 30 min at 37 °C. Briefly, 100 µl of 3, 5-dinitrosalicylic acid (DNS) was added and boiled for 10 min at 95 °C to stop the reaction. The absorbance was read at 540 nm using Multiplate Reader (Multiskan Thermo Scientific, USA).

2.8.2. α-Glucosidase inhibition assay

The inhibition was assessed using the slightly modified method as described by Madhusudhan and Kirankumar [21]. Each well of a 96-well plate contained a reacting mixture of 50 µl phosphate buffer (100 mM, pH = 6. 8), 20 µl alpha-glucosidase (1 U/ml), and 20 µl of varying concentrations of AgNPs and acarbose as standard pre-incubated for 15 min at 37 °C. Further, 20 µl 4-Nitrophenyl β-D-glucopyranoside (P-NPG, substrate) (5 mM) was added and followed by an incubation at 37 °C for 20 min. The reaction was stopped by adding 50 µl Na_2CO_3 (0.1 M) and the absorbance of p-nitrophenol released was read at 405 nm using a multiplate reader (Multiskan, Thermo Scientific, USA). Furthermore, the kinetic mechanism of the nanoparticle was evaluated using the IC_{50} value concentration of the nanoparticles in the presence of graded concentration of the substrate. The reaction was evaluated using the same condition as stated above.

2.9. Bacterial growth inhibition assay

The antibacterial potency of the bio-fabricated AgNPs was evaluated against certain clinical-relevant bacterial isolates, including *Staphylococcus aureus, Escherichia coli, Serratia marcescens, Bacillus cereus, Pseudomonas aeruginosa* and *Salmonella enterica* using a microdilution assay [20, 22]. An inoculum of each test bacterial strain was grown in nutrient broth for 24 h and adjusted to 0.5 McFarland standard in 5.0 ml of phosphate buffer (PBS). This was again diluted in 1:50 PBS to obtain a 1:20 in brain heart infusion broth (BHI) by adding 250 µl of (1:50) and 750 µl of BHI. For the test samples, 100 µL each of 100 and 50 µg/ml concentrations of AgNPs was pre-mixed with 100 µL of BHI in a sterile 96-well microtitre plate. Thereafter, 100 µl of gradient concentrations of the nanoparticles was inoculated with 100 µl of the test isolate. In the control sample, the bacterial suspension (100 µl) was inoculated with 100 µl of sterile distilled water without the inclusion of AgNPs. The plates were incubated with shaking at 37 °C for 24 h. The plates were monitored for clarity/turbidity and further supported with the addition of 40 µl of 0.2 mg/ml iodonitrotazolium chloride (INT) for colour change after 30 min incubation. Thereafter, the growth of bacterial isolates was considered as optical density and read at a wavelength of 530 nm. All the experiments were carried out in triplicate and the percentage growth inhibition was calculated.

2.10. Cytotoxicity and viability assays

Cytotoxicity was evaluated using MTT [3-(4,5-dimethylthiazol-2-yl)-2,5-diphenyltetrazolium bromide] and the CytoTox Glo™ kit from Promega. HaCaT cells were seeded in 96-well plates at a concentration of 2×10^4 cells per well. The cells were treated with varying concentrations of the AgNPs while including tamoxifen and cisplatin (as positive controls) for 24 h. After treatment, 20 µl MTT (0.5 mg/ml) was added to each well and allowed to further incubate in the CO_2 incubator for 4 h. Hereafter, the MTT containing medium in each well was discarded and replaced with 100 µl DMSO to dissolve the blue formazan crystals where after absorbance was read at 570 nm in a multi-well ELISA microplate reader. The Cyto Tox Glo™ luminescent assay measures proteases that leaked from compromised cell membranes of dead cells into the culture media. The Manufacturer's protocol instruction was strictly adhered to for the determination of the cell viability (Promega).

2.11. Statistical analysis

The results were analyzed using Two-Way ANOVA followed by post hoc Tukey's multiple comparisons test using GraphPad Prism software version 6.05 for Windows (GraphPad Software, La Jolla California USA (www.graphpad.com). A P value of less than 0.05 was considered significant.

3. Results and discussion

3.1. Photo aided synthesis of Annona muricata-AgNPs

Green bio-fabrication of AgNPs and its *in vitro* biological evaluation was the major focus of this study. The change in colour from colourless to dark brown after the addition of the aqueous leaf extract of *A. muricata* to the silver salt solution, confirmed the reduction of Ag^+ to zero valent Ag metal (Figure 1). Several earlier studies have reported dark brown colour for the formation of silver nanoparticles [23, 24]. However, phenols, alkaloids, flavonoids, terpenoids, and tannins have been previously reported among the phytoconstituents present in the leaf of *A. muricata* [25]. Some of these phytochemicals have been shown to be responsible for the formation of nanoparticles by causing the excitation of surface plasmon resonance (SPR) of the particles [26, 27, 28]. Photo induced synthesis of the AgNPs as presented in this study has shown that introduction of heat is not necessary as reported by previous studies [15, 29].

3.2. Physicochemical characterization of synthesized AgNPs

The UV-visible spectral SPR peak of AgNPs was detected at about 420 nm, a typical absorbance band of silver nanoparticles as presented in Figure 2 [11,30]. To further understand the specific chemical

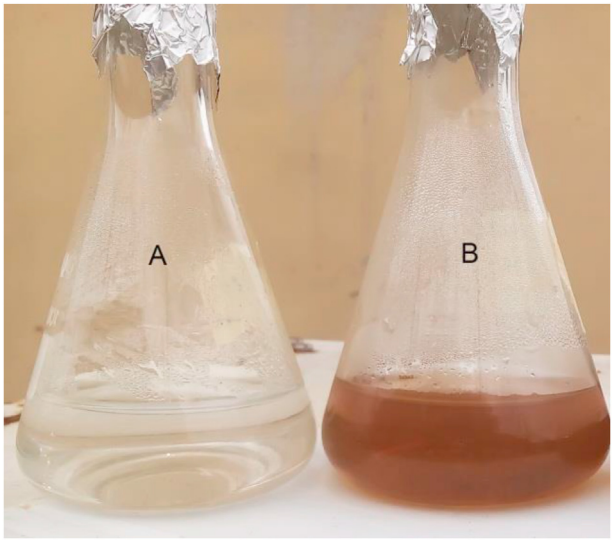

Figure 1. Green synthesis of silver nanoparticle using aqueous leaf extract of *A. muricata.* The change of colourless solution of silver nitrate (A) to dark brown solution (B) is an indication of bio-reduction of Ag^+ to AgNPs in the presence of aqueous leaf extract of *A. muricata* under light ray for 30 min.

constituents in the extract as well as those that might be participating in the reduction and stabilization of the nanoparticles, the FTIR spectroscopy was employed. The FTIR analysis was carried out on both the extract and the dried pellets of the AgNPs. Apparent changes in the spectra of the leaf extract and synthesized AgNPs were observed (Figure 3). The FTIR spectrum of the leaf extract (Figure 3a) showed bands at 428, 1017, 1436, 1619, 2919, and 3212 cm^{-1}. The peak positioned at 1017 cm^{-1} relates to vibration from a single bond between carbon and nitrogen (C–N) that can be assigned to aliphatic amines. This assignment was corroborated by the two weak bands at 1436 and 1619 cm^{-1}, both of which are assignable to proteins. The 2916 cm^{-1} band further confirms the presence of nitrogen-containing functional groups. A more pronounced band, however, appeared at about 3212 cm^{-1}, signifying the presence of hydroxyl functional groups that may belong to polyphenols in general as earlier mentioned. Hence, it can be inferred that polyphenols such as phenols and flavonoids may participate in the reduction process that led to the successful bio-fabrication of the particles that were capped with nitrogen-bearing molecules such as amines or proteins. Similarly, the FTIR spectrum of the silver nanoparticles (Figure 3b) biosynthesized from the aqueous leaf extract shows some common functional groups with enhanced intensity. The band at 1641 and 3296 cm^{-1} can be ascribed to some free amide I and hydroxyl groups of phytochemicals present [31]. The 1619 and 1641 cm^{-1} bands in both leaf extract and the AgNPs further confirm that the structure of proteins was not altered after reduction [32]. This further buttress the fact that proteins and various polyphenols served as bioreductants from the extract and equally responsible for stabilizing the bio-fabricated AgNPs. A previous study indicated the involvement of alcohol amines for the synthesis of silver nanoparticles from *Streptomyces* sp [33]. The FITR peaks obtained in this study are closely related to the observed peaks in earlier studies using the leaf and fruit extracts of *A. muricata* [15, 16, 34]. This confirms that similar phytochemicals are responsible for the synthesis of the AgNPs by the plant irrespective of the mode of synthesis.

The crystal structure of the biosynthesized AgNPs was examined with the aid of an X-ray Diffractometer. Based on the XRD pattern (Figures 4a and 4b), it shows that the AgNPs were in polycrystalline form. The two theta degrees were approximately 38, 44, 64, and 78 which correspond well with the planes (111, 200, 220, and 311 respectively) of pure crystalline silver [35]. In addition to the XRD result, selected area electron diffraction (SAED) assessment further confirms the crystal nature of the AgNPs. The bright rings in the SAED agree with the planes when the diameters of the rings are considered (Figure 4b).

Figures 5a and b show the TEM micrographs accompanied by particle size distribution (Figure 5c) of the AgNPs. The mean diameter of the AgNPs was found to be approximately 35 nm. Most of the seeds were in the spherical forms as can be observed in Figure 5 which, further shows that both AgNPs were monodispersed with a spherical shape. The sizes of

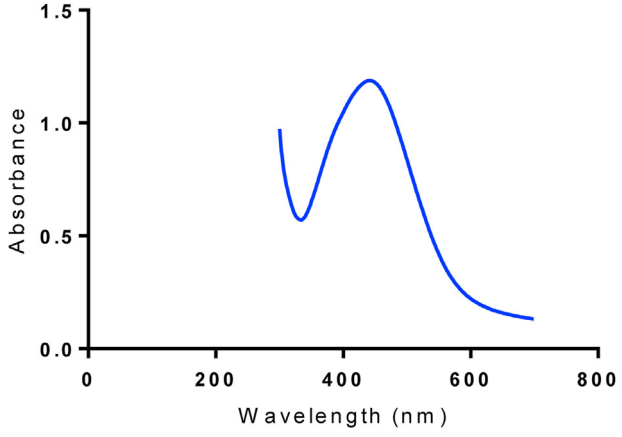

Figure 2. UV-visible spectrum of synthesized AgNPs using aqueous leaf extract of *A. muricata* at 420 nm.

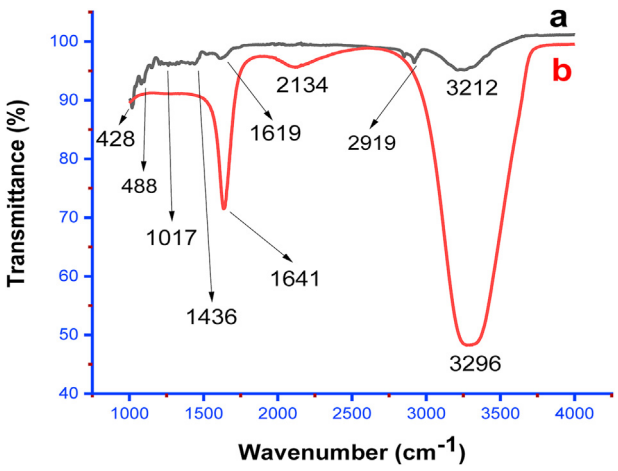

Figure 3. FTIR spectral of powdered (a) leaf of *A muricata* and (b) *A. muricata*-AgNPs.

the synthesized AgNPs using various plants in previous studies have been found to be in the range of 20–53 nm [15, 16, 34]. In addition, as shown in Figure 4b, jellylike substances can be seen surrounding the particles. This may be related to biomolecules serving as the stabilizing agents to the fabricated AgNPs. To further confirm the formation of AgNPs, the EDS was employed. The EDS spectrum in Figure 6 shows an arrow pointing to the region where clusters of silver atoms were detected by the analysis. Previously, the presence of silver atoms has been shown to imply the confirmation of the successful fabrication of AgNPs [36]. The EDS also shows the presence of other elements like carbon from the phytochemicals in the precursor plant extract and copper from the copper grid used in the sample preparation for TEM [37]. The size distribution, shape, assembly, stability and aggregation of nanoparticles depend on the nature of preparation and reducing/capping agents [38]. Phase behaviour of nanoparticles is, among other important factors used to evaluate the propriety of the particles before applications. Interestingly, light scattering is a special technique that gives an idea of the hydrodynamic size of the particles. Through DLS measurement, the electric charge around the surface of nanoparticles is also understood [39]. DLS measurement of the particles indicated that the majority of the particles are of 86.78 nm size with a polydispersity index (PDI) of 0.329. The PDI measures the degree of non-uniformity of size distribution of particles, which is the ratio of weight average and the number average molecular weight. The normal range of PDI is between 0.05-0.7 while the value beyond 0.7 indicates undesirable broad particle size distribution [40]. The zeta potential value of -27.2 mv (Figure 7) means that a large negative ion exists on the surface of the particles. It further implies that a strong repulsive force is present in the assembly of ions because of the high negative zeta potential. The strong repulsive force, however, reduces the possibility of aggregation and enhances the stability of nanoparticles [41]. The aggregation in synthesized nanoparticles induces instability in the particles and hence obliterates its essential functional properties [42]. The DLS, PDI and zeta potential values of the work of Meenakshisundaram et al. [29] and Gavamukulya et al. [16] are different from the values obtained in this study. The disparity in values is likely to be due to the differences in the preparation of the nanoparticles.

3.3. Antioxidant activities of synthesized AgNPs

The *in vitro* free radical scavenging ability of the AgNPs was evaluated using DPPH and $ABTS^{+}$ radicals, respectively. The assays are common endpoint methods of determining the antioxidant capacity of various compounds. DPPH is a stable radical that readily accepts hydrogen or an electron from the antioxidant agent that bleaches purple to a golden yellow colour. The synthesized AgNPs effectively scavenged DPPH in a

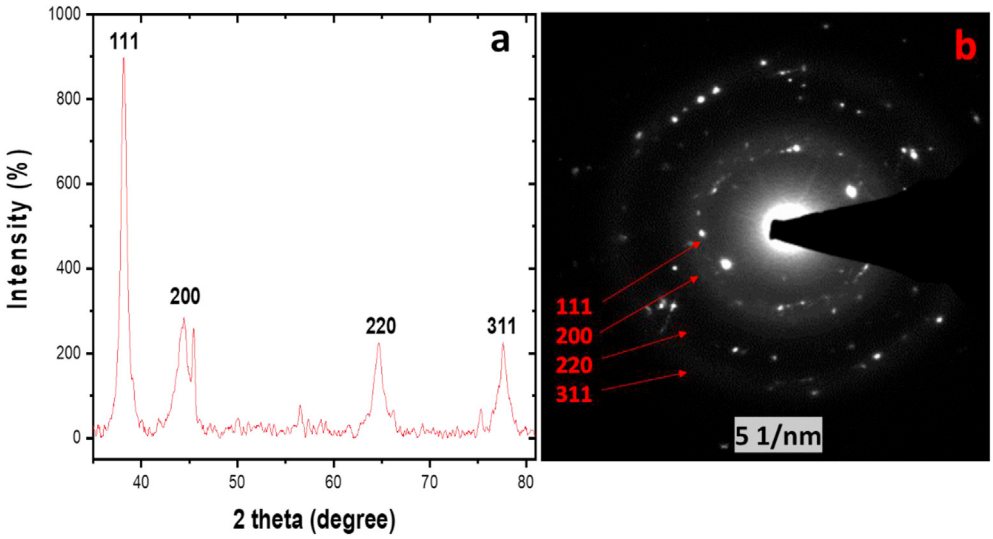

Figure 4. XRD (a) and SAED (b) profiles of *A. muricata*-AgNPs.

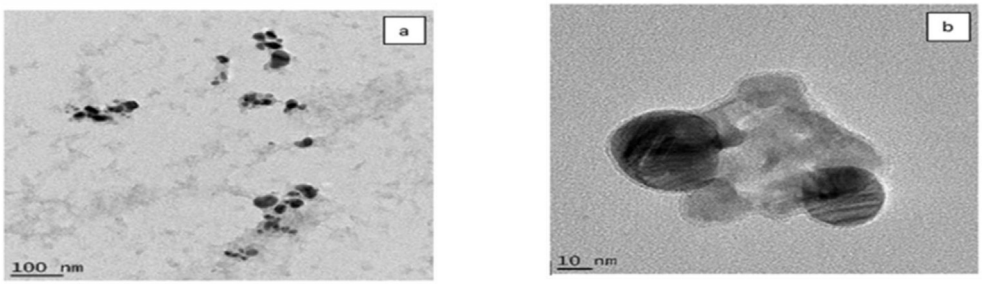

Figure 5. TEM images (a, b) depicted the size and shape of the synthesized aqueous *A. muricata* leaf extract-induced AgNPs.

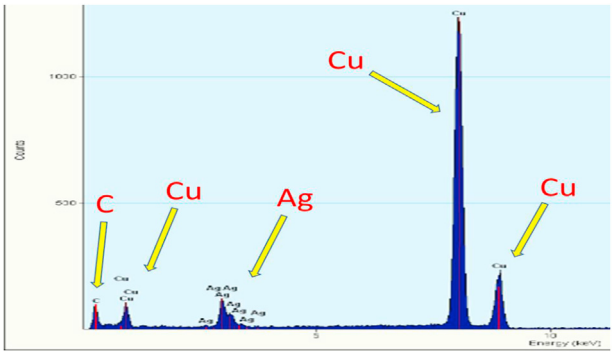

Figure 6. EDS of aqueous *A. muricata* leaf extract-induced AgNPs showing the elemental composition.

dose-dependent manner with IC_{50} values of 51.80 μg/ml against standard Trolox with 5.25 μg/ml (Table 1). The nanoparticles scavenged the ABTS radical with IC_{50} value of 30.78 μg/ml as presented in Table 1. The lower IC_{50} value against ABTS comparatively to DPPH implies that the AgNPs is a stronger scavenger of ABTS radical. The antioxidant property of the nanoparticles was borne out of the interaction of antioxidant agents in the aqueous leaf extract that may be involved in the bio-reduction and subsequent capping of the silver salt. These phytochemicals are proposed to have conferred the antioxidant property onto the bio-fabricated nanoparticles. Antioxidants are important molecules needed to counteract the induction of excessive free radicals in an aerobic organism and consequently protect against induced oxidative stress-related ailments [43]. Previous studies have reported the ability of AgNPs fabricated using leaf extracts prepared from *C. roseus* and *P. granatum* as good scavengers of free radicals [8, 44]. Antioxidant property of nanoparticles has been reported to have a comparative advantage over the traditional antioxidant delivery system such as encapsulated protection of antioxidant agent, elevated bioavailability, targeted and controlled delivery [45].

3.4. Lipid peroxidation inhibitory activity of synthesized AgNPs

Lipid peroxidation is the product of radicals' assault on the lipid membrane with far-reaching implications on the functionality of the cells. The cell functions are impaired due to the disruption of the cell membrane assembly leading to prejudiced membrane fluidity, permeability, ion transport modification, and eventual inhibition of metabolic processes [46, 47]. The TBARS assay is a commonly used method of determination of lipid peroxidation through spectrophotometric evaluation of TBARS-MDA adducts [20]. The silver nanoparticles show dose-dependent inhibition of Fe^{2+}-induced lipid peroxidation in both liver S9- and chicken egg yolk homogenates (Table 2). Each level of concentration of the particles displays a better/higher protection against the induced lipid peroxidation when using the egg yolk as compared to the liver homogenate results. This result shows that the antioxidant components and enzymes inherent in the liver homogenate did not boost the activity of the nanoparticles against induced lipid peroxidation. In addition, the nanoparticles protect the egg yolk from peroxidation

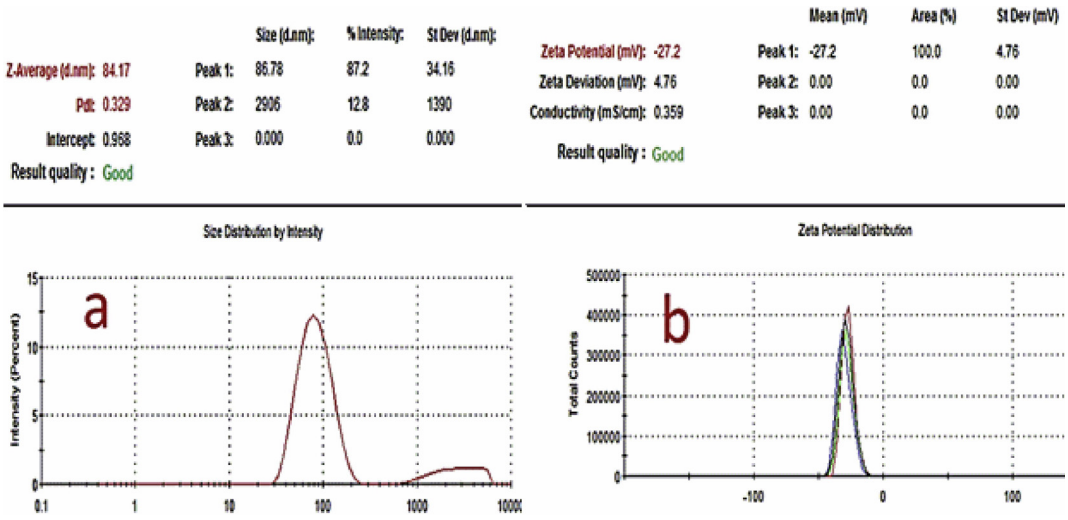

Figure 7. Dynamic light scattering measurement showing (a) the average hydrodynamic size (HDS) of 84.17 nm and a polydisperity index (PDI) of 0.329 and (b) showing the zeta potential value of -27.2 mV.

Table 1. *In vitro* Antioxidant (DPPH and ABTS), Antidiabetic (α-amylase and α-glucosidase) and cytotoxicity potential of aqueous *A. muricata* leaf extract-induced AgNPs.

IC_{50} (μg/ml)	DPPH	ABTS	α-amylase	α-glucosidase	Cytotoxicity
AgNPs	51.80 ± 3.14	30.78 ± 1.10	0.90 ± 0.01***	3.32 ± 0.32***	57.37 ± 3.66
Trolox	5.26 ± 0.04***	3.74 ± 0.01***			
carbose			10.20 ± 0.05	610.65 ± 4.27	
Cisplatin					3.12 ± 0.54***
Tamoxifen					22.00 ± 1.02***

The results are expressed as mean ± SD of three different independent experiments ($n = 3$). The results with superscript *** indicate significantly difference at $P < 0.0001$. Trolox, acarbose, cisplatin and tamoxifen are standards used for different experiments.

Table 2. Inhibition of Fe^{2+}-induced lipid peroxidation in egg yolk and rat liver homogenates by *A. muricata* leaf extract-induced AgNPs.

Concentration (μg/ml)	Percentage Inhibition	
	Egg yolk	Liver
350.0	66.37 ± 1.22	61.13 ± 0.20
175.0	58.29 ± 0.59	47.97 ± 0.52
87.5	48.67 ± 1.60	40.16 ± 0.23
43.8	45.58 ± 4.51	39.36 ± 0.31

The results are expressed as mean ± SD of three different independent experiments ($n = 3$).

effectively, notwithstanding the readily peroxidized high content of polyunsaturated lipids in egg yolk with low components of antioxidant booster when compared with the liver [20].

3.5. *In vitro* antidiabetic potential of synthesized AgNPs

Alpha-amylase and Alpha-glucosidase inhibitors are agents that can be used to effectively control postprandial hyperglycemia-linked Type II diabetes mellitus [48]. The silver nanoparticles significantly ($P < 0.0001$) inhibited both α-amylase and α-glucosidase with IC_{50} values of 0.90 and 3.32 μg/ml, respectively, when compared with the standard, acarbose with IC_{50} values of 10.20 and 610.65 μg/ml respectively (Table 1). The biosynthesized AgNPs was significantly potent against both enzymes when compared with the standard acarbose. Several studies have reported the anti-diabetic activity of AgNPs using the inhibitory activities against the two enzymes. However, to the best of our knowledge, none of the reported activities have been as strong as what is being reported in this study [44, 49, 50]. This result implies that *A. muricata*-AgNPs as prepared in this study could be a strong anti-diabetic entity for the future development of a safe and physiologically functional drug. Furthermore, the alpha-glucosidase inhibitory kinetic study shows that the particles inhibited the enzyme through non-competitive inhibition (Figure 8). This implies that the particles inhibited the enzyme by binding to the other site of the enzyme apart from the active site and enzyme-substrate complex. In addition, the particles have a strong affinity to the other site of the enzyme apart from the active site and do not interfere with substrate binding but prevent catalytic step. The synthesis of eco-friendly nanoparticles has become effective and emerging treatment of diabetes mellitus and its associated legacy and complication [51].

3.6. Antimicrobial activities of synthesized AgNPs

The AgNPs inhibited the growth of bacterial isolates at both concentrations of 100 and 50 μg/ml. The maximal inhibition was achieved for all the isolates at 100 μg/ml. *S. aureus* was the most sensitive to the nanoparticles with 61.29% inhibition followed by *S. marcescens and P. aeruginosa* with 59.34 and 54.42% inhibition respectively at 50 μg/ml. The least sensitive to the AgNPs at 50 μg/ml were *B. cereus* and *Salmonella* sp with 26.21 and 21.44% inhibition (Figure 9). Silver nanoparticles have been reported to display strong antibacterial property against both Gram positive and negative bacteria. Silver nanoparticles synthesized using *Punica granatum*, *Prosopis cineraria* leaf, *Ananas comosus* peel extract, *Rosmarinus officinalis* leaf and Cocoa pod husk extract have been reported to exhibit considerable antibacterial activities in agreement with the present study [5, 6, 9, 44, 52]. However, several mechanisms have been attributed to the antibacterial effect of AgNPs. These mechanisms include, but are not limited to the attachment to and disruption of

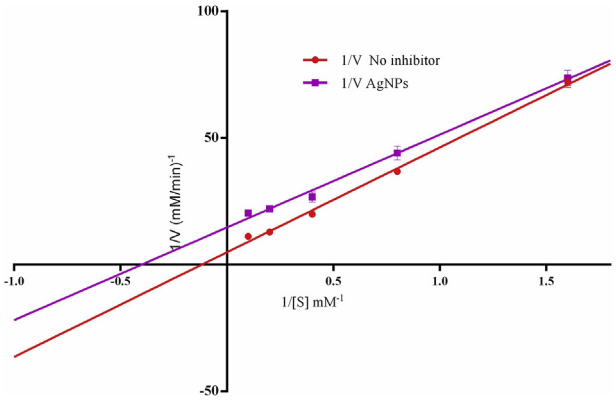

Figure 8. Kinetic inhibition of α-glucosidase by aqueous *A. muricata* leaf extract-induced AgNPs.

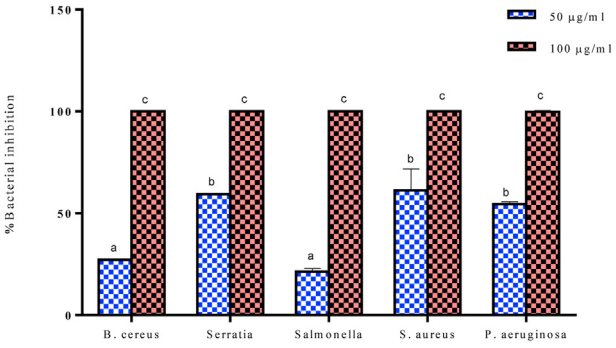

Figure 9. Antimicrobial potential of aqueous *A. muricata* leaf extract-induced AgNPs using microdilution assay. Each bar represents mean ± SD of triplicate experiments. Bar not sharing a common alphabet (a–c) are significantly different ($P < 0.05$).

the bacterial cell membrane, disruption of respiratory function and DNA replication, induced ROS, derangement of the glycolytic pathway and modulation of cellular signaling by dephosphorylating putative key peptide substrates on tyrosine residues [6, 8, 53].

3.7. Cytotoxicity potential of synthesized AgNPs

The MTT assay and CytoTox Glo™ kit (Promega) were used to determine the cytotoxicity and the viability potential of the synthesized nanoparticles compared to standard anti-cancer drugs, tamoxifen and cisplatin against the HaCaT cell line, respectively. The two assays results revealed the *in vitro* cytotoxicity ability of the nanoparticles against the HaCaT cell line. The IC_{50} cytotoxicity value of the nanoparticles was found to be 57.37 µg/ml compared to that of cisplatin (3.12 µg/ml) and tamoxifen (22.00 µg/ml) as presented in Table 1 and Figure 10. Previous similar studies have shown the cytotoxicity effect of AgNPs in different cell lines [5, 6, 39]. The cytotoxicity of AgNPs has been related to the active interaction between the phytoconstituents and the silver atoms with functional groups of intracellular proteins, nitrogen bases and phosphate groups in the DNA [6]. In addition, AgNPs cytotoxic effect can also be ascribed to cellular damage, induction of a cascade of immunological effects and electrostatic attraction between the cell and AgNPs [54]. Generation of reactive oxygen species (ROS) leading to the induction of oxidative stress linked release of pro-inflammatory protease, caspase induction and eventual cell death through apoptosis is another mechanism of nanoparticles induced cytotoxicity [55]. Furthermore, the AgNPs did not induce caspase-3 enzyme (result not shown), the final executioner enzyme for the induction of apoptosis. This is contrary to the previous finding that reported activation of apoptosis of the nanoparticles in NSCLC cell lines using different assay apart from the caspase-3 induction [29]. This implies either that the cells had already gone beyond apoptosis stage at the period of evaluation or the HaCaT cell line is not sensitive to the apoptotic effect induced by the nanoparticles.

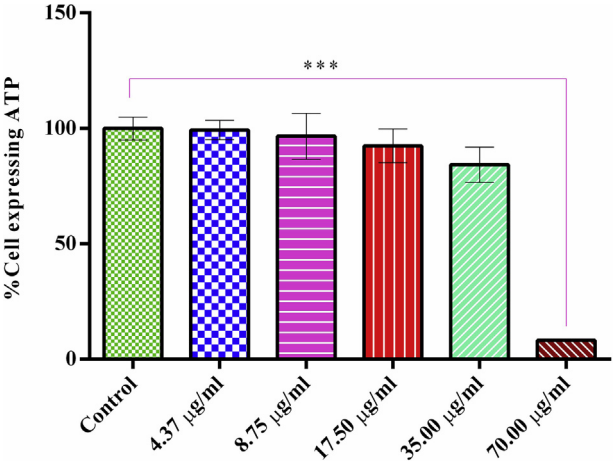

Figure 10. Effect of aqueous *A. muricata* leaf-induced AgNPs on HaCaT cell viability (ATP expressing cells) using CytoTox™ kit from Promega. Each bar represents mean ± SD of three different independent experiments and ***$P < 0.0001$ shows level of significance.

4. Conclusion

The synthesized AgNPs using the leaf extract of *A. muricata* showed strong *in vitro* antioxidant activity, lipid peroxidation inhibition, effective *in vitro* anti-diabetic and antimicrobial activities as well as cytotoxicity against the HaCaT cell line. These arrays of unique medicinal bio-active potential can position the AgNPs as an agent for future biomedical application, most especially as an anti-diabetic agent where its activity was most pronounced. Future *in vivo* studies would further establish the possibility of its biomedical exploitation.

Declarations

Author contribution statement

J. A. Badmus: Conceived and designed the experiments; Performed the experiments; Analyzed and interpreted the data; Wrote the paper.

S. A. Oyemomi, E. A. Adebayo: Performed the experiments; Analyzed and interpreted the data; Wrote the paper.

O. T. Adedosu, T. A. Yekeen, M. A. Azeez: Conceived and designed the experiments; Analyzed and interpreted the data; Contributed reagents, materials, analysis tools or data.

A. Lateef: Conceived and designed the experiments; Contributed reagents, materials, analysis tools or data; Wrote the paper.

U. M. Badeggi, S. Botha: Performed the experiments; Contributed reagents, materials, analysis tools or data.

A. A. Hussein, J. L. Marnewick: Analyzed and interpreted the data; Contributed reagents, materials, analysis tools or data; Wrote the paper.

Funding statement

This research did not receive any specific grant from funding agencies in the public, commercial, or not-for-profit sectors.

Competing interest statement

The authors declare no conflict of interest.

Additional information

No additional information is available for this paper.

References

[1] M. Govindappa, B. Hemashekhar, M.-K. Arthikala, R.V. Ravishankar, Y.L. Ramachandra, Characterization, antibacterial, antioxidant, antidiabetic, anti-inflammatory and antityrosinase activity of green synthesized silver nanoparticles using *Calophyllum tomentosum* leaves extract, Results Phys 9 (2018) 400–408.

[2] B. Nair, T. Pradeep, Coalescence of nanoclusters and formation of submicron crystallites assisted by Lactobacillus strains cryst, Growth Des 2 (2002) 293–298.

[3] K.B. Narayanan, N. Sakthivel, Biological synthesis of metal nanoparticles by microbes, Adv. Colloid Interface Sci. 156 (2010) 1–13.

[4] K. Chaloupka, Y. Malam, A.M. Seifalian, Nanosilver as a new generation of nanoproduct in biomedical applications, Trends Biotechnol. 28 (2010) 580–588.

[5] G. Das, J.K. Patra, T. Debnath, A. Ansari, H.-S. Shin, Investigation of antioxidant, antibacterial, antidiabetic, and cytotoxicity potential of silver nanoparticles synthesized using the outer peel extract of *Ananas comosus* (L.), PloS One 14 (2019), e0220950.

[6] U. Jinu, M. Gomathi, I. Saiqa, N. Geetha, G. Benelli, P. Venkatachalam, Green engineered biomolecule-capped silver and copper nanohybrids using Prosopis cineraria leaf extract: enhanced antibacterial activity against microbial pathogens of public health relevance and cytotoxicity on human breast cancer cells (MCF-7), Microb. Pathog. 105 (2017) 86–95.

[7] T. Kayalvizhi, S. Ravikumar, P. Venkatachalam, Green synthesis of metallic silver nanoparticles using Curculigo orchioides rhizome extracts and evaluation of its antibacterial, larvicidal, and anticancer activity, J. Environ. Eng. 142 (2016) C4016002.

[8] S. Hanady, A. Al-Shmgani, W.H. Mohammed, G.M. Sulaiman, A.H. Saadoon, Biosynthesis of silver nanoparticles from *Catharanthus roseus* leaf extract and assessing their antioxidant, antimicrobial, and wound-healing activities, Artif. Cell Nanomed. B. 45 (2017) 1234–1240.

[9] M. Ghaedi, M. Yousefinejad, M. Safarpoor, H.Z. Khafri, M.K. Purkait, *Rosmarinus officinalis* leaf extract mediated green synthesis of silver nanoparticles and investigation of its antimicrobial properties, J. Ind. Eng. Chem. 31 (2015) 167–172.

[10] A.R. Vilchis-Nestor, V. Sanchez-Mendieta, M.A. Camacho-Lopez, R.M. Gomez-Espinosa, M.A. Camacho-Lopez, J.A. Arenas-Alatorre, Solventless synthesis, and optical properties of Au and Ag nanoparticles using *Camellia sinensis* extract, Mater. Lett. 62 (2008) 3103–3105.

[11] B. Ajitha, K.R.Y. Ashok, R.P. Sreedhara, Green synthesis and characterization of silver nanoparticles using *Lantana camara* leaf extract, Mater. Sci. Eng. 49 (2015) 373–381.

[12] S.M. Abdul Wahab, I. Jantan, M.A. Haque, L. Arshad, Exploring the leaves of *Annona muricata* L. As a source of potential anti-inflammatory and anticancer agents, Front. Pharmacol. 9 (2018) 661.

[13] Y. Gavamukulya, F. Wamunyokoli, H.A. El-Shemy, *Annona muricata*: is the natural therapy to most disease conditions including cancer growing in our backyard? A systematic review of its research history and future prospects, Asian Pac. J. Trop. Med. 10 (2017) 835–848.

[14] A.I. Yajid, H.S. Ab-Rahman, M.P.K. Wong, W.Z. Wan Zain, Potential benefits of *Annona muricata* in combating cancer: a review, Malays. J. Med. Sci. 25 (2018) 5–15.

[15] S.B. Santhosh, R. Yuvarajan, D. Natarajan, *Annona muricata* leaf extract-mediated silver nanoparticles synthesis and its larvicidal potential against dengue, malaria and filariasis vector, Parasitol. Res. 114 (2015) 3087–3096.

[16] Y. Gavamukulya, E.N. Maina, A.M. Meroka, E.S. Madivoli, H.A. El-Shemy, F. Wamunyokoli, G. Magoma, Green synthesis and characterization of highly stable silver nanoparticles from ethanolic extracts of fruits of *Annona muricata*, J. Inorg. Organomet. Polym. Mater. 30 (2020) 1231–1242.

[17] T.A. Yekeen, M.A. Azeez, A. Lateef, T.B. Asafa, I.C. Oladipo, J.A. Badmus, S.A. Adejumo, A.A. Ajibola, Cytogenotoxicity potentials of cocoa pod and bean mediated green synthesized silver nanoparticles on *Allium cepa* cells, Caryologia 70 (2017) 366–377.

[18] J.K. Kim, J.H. Noh, S. Lee, J.S. Choi, H. Suh, H.Y. Chung, Y.O. Song, W.C. Choi, The first total synthesis of 2, 3, 6-tribromo-4, 5-dihydroxybenzyl methyl ether (TDB) and its antioxidant activity, Bull. Kor. Chem. Soc. 23 (2002) 661–662.

[19] B. Moldovan, L. David, M. Achim, S. Clichici, G.A. Filip, A green approach to phytomediated synthesis of silver nanoparticles using *Sambucus nigra* L. fruits extract and their antioxidant activity, J. Mol. Liq. 221 (2016) 271–278.

[20] J.A. Badmus, O.T. Adedosu, J.O. Fatoki, V.A. Adegbite, O.A. Adaramoye, O.A. Odunola, Lipid peroxidation inhibition and antiradical activities of some leaf fractions of mangifera indica, Acta Pol. Pharm. 68 (2011) 23–29.

[21] T. Madhusudhan, H. Kirankumar, *In-vitro* α-amylase and α-glucosidase inhibitory activity of *Adiantum caudatum* Linn. and *Celosia argentea* Linn. extracts and fractions, Indian J. Pharmacol. 47 (2015) 425–429.

[22] J.R. Zgoda, J.R. Porter, A convenient microdilution method for screening natural products against bacterial and fungi, Pharm. Biol. 39 (2001) 221–225.

[23] S. Ahmed, S.M. Ahmad, B.L. Swami, S. Ikram, Green synthesis of silver nanoparticles using azadirachta indica aqueous leaf extract, J. Rad. Res. Appl. Sci. 9 (2016) 1–7.

[24] K. Abhishek, J. Sanyog, C.B. Uttam, Green and rapid synthesis of anticancerous silver nanoparticles by saccharomyces boulardii and insight into mechanism of nanoparticle synthesis, Biotechnol. Green Chem. 2013 (2013).

[25] A.V. Coria-Téllez, E. Montalvo-Gónzalez, E.M. Yahia, E.N. Obledo-Vázquez, Annona muricata: a comprehensive review on its traditional medicinal uses, phytochemicals, pharmacological activities, mechanisms of action and toxicity, Arabian J. Chem. 11 (2018) 662–691.

[26] A.O. Dada, F.A. Adekola, F.E. Dada, A.T. Adelani-Akande, M.O. Bello, C.R. Okonkwo, A.A. Inyinbor, A.P. Oluyori, A. Olayanju, K.O. Ajanaku, C.O. Adetunji, Silver nanoparticle synthesis by *Acalypha wilkesiana* extract: phytochemical screening, characterization, influence of operational parameters, and preliminary antibacterial testing, Heliyon 5 (2019), e02517.

[27] G. Marslin, K. Siram, Q. Magbool, R.K. Selvakesan, D. Kruszka, P. Kachlicki, G. Franklin, Secondary metabolites in the green synthesis of metallic nanoparticles, Materials 12 (2019) 806.

[28] K.S. Siddiqi, A. Husen, R.A.K. Rao, A review of biosynthesis o silver nanoparticles and their biocidal properties, J. Nanobiotechnol. 16 (2018) 14.

[29] S. Meenakshisundaram, V. Krishnamoorthy, Y. Jagadeesan, R. Vilwanathan, A. Balaiah, *Annona muricata* assisted biogenic synthesis of silver nanoparticles regulates cell cycle arrest in NSCLC cell lines, Bioorg. Chem. 95 (2020) 103451.

[30] R.M. Elamawi, R.E. Al-Harbi, A.A. Hendi, Biosynthesis and characterization of silver nanoparticles using *Trichoderma longibrachiatum* and their effect on phytopathogenic fungi, Egyptian J. Biol. Pest Control 28 (2018) 28.

[31] A. Barth, Infrared spectroscopy of proteins, BBA-Bioenergetics. 17167 (2007) 1073–1101.

[32] A. Pugazhendhi, D. Prabakar, J.M. Jacob, I. Karuppusamy, R.G. Saratale, Synthesis and characterization of silver nanoparticles using *Gelidium amansii* and its antimicrobial property against various pathogenic bacteria, Microb. Pathog. 114 (2018) 41–45.

[33] P.S. Kumar, C. Balachandran, V. Duraipandiyan, D. Ramasamy, S. Ignacimuthu, N.A. Al-Dhabi, Extracellular biosynthesis of silver nanoparticles using Streptomyces sp. and its antibacterial and cytotoxic properties, Appl. Nanosci. 5 (2014) 169–180.

[34] S.B. Santhosh, C. Ragavendran, D. Natarajan, Spectral and HRTEM analyses of Annona muricata leaf extract mediated silver nanoparticles and its Larvicidal efficacy against three mosquito vectors Anopheles stephensi, Culex quinquefasciatus, and Aedes aegypti, J. Photochem. Photobiol., B 153 (2015) 184–190.

[35] K. Jyoti, M. Baunthiyal, A. Singh, Characterization of silver nanoparticles synthesized using *Urtica dioica* Linn. Leaves and their synergistic effects with antibiotics, J. Rad. Res. App. Sci. 9 (2016) 217–227.

[36] J. Kero, B.V. Sandeep, P. Sudhakar, Synthesis, Characterization, and evaluation of the antibacterial activity of *Allophylus serratus* leaf and leaf derived callus extracts mediated silver nanoparticles, J. Nanomater. 2017 (2017).

[37] N. Berahim, W.J. Basirun, B.F. Leo, M.R. Johan, Synthesis of bimetallic gold-silver (Au-Ag) nanoparticles for the catalytic reduction of 4-nitrophenol to 4-aminophenol, Catalysts 8 (2018) 412.

[38] I. Khan, K. Saeed, I. Khan, Nanoparticles: properties, applications and toxicities, Arabian J. Chem. 12 (2019) 908–931.

[39] T. Varadavenkatesan, E. Lyubchik, S. Pai, A. Pugazhendhi, R. Vinayagam, R. Selvaraj, Photocatalytic degradation of Rhodamine B by Zinc oxide nanoparticles synthesized using the leaf exract of *Cyanometra ramiflora*, J. Photochem. Photobiol. B Biol. 199 (2019) 111621.

[40] M. Danaei, M. Dehghankhold, S. Ataei, F. Hasanzadeh Davarani, R. Javanmard, A. Dokhani, S. Khorasani, M.R. Mozafari, Impact of particle size and polydispersity index on the clinical applications of lipidic nanocarrier systems, Pharm. Times 10 (2018) 57.

[41] S. Samimi, N. Maghsoudnia, R.B. Eftekhari, F. Dorkoosh, Lipid-based nanoparticles for drug delivery systems, in: S.S. Mohapatra, S. Ranjan, N. Dasgupta, R.K. Mishra, S. Thomas (Eds.), Characterization and Bology of Nanomaterials for Drug Delivery, Elsevier B.V., Netherlands, 2019, pp. 47–76.

[42] R. Vinayagam, T. Varadavenkatesan, R. Selvaraj, Green synthesis, structural characterization and catalytic activity of silver nanoparticles stabilized with *Bridelia retusa* leaf extract, Green Process. Synth. 7 (2018) 30–37.

[43] B.L. Tan, M. Norhaizan, W.-P. Liew, H.S. Rahman, Antioxidant and oxidative stress: a mutual interplay in age-related diseases, Front. Pharmacol. 9 (2018) 1162.

[44] R.G. Saratale, H.S. Shin, G. Kumar, G. Benelli, D.-S. Kim, G.D. Saratale, Exploiting antidiabetic activity of silver nanoparticles synthesized using *Punica granatum* leaves and anticancer potential against human liver cancer cells (HepG2), Artif. Cell Nanomed. B. 46 (2018) 211–222.

[45] I. Khalil, W.A. Yehye, A.E. Etxeberria, A.A. Alhadi, S.M. Dezfooli, N.B.-M. Julkapli, W.J. Basirun etc, Nanoantioxidants: recent trends in antioxidant delivery applications, Antioxidants 9 (2019) 24.

[46] J.A. Badmus, O.A. Odunola, T.A. Yekeen, A.M. Gbadegesin, J.O. Fatoki, M.O. Godo, K.S. Oyebanjo, D.C. Hiss, Evaluation of antioxidant, antimutagenic, and lipid peroxidation inhibitory activities of selected fractions of *Holarrhena floribunda* (G. Don) leaves, Acta Biochim. Pol. 60 (2013) 435–442.

[47] K. Pavithra, U.V.V. Sathibabu, S. Ganapathy, S. Vadivukkarasi, Therapeutic potentiality of *Kedrostis foetidissima* (Jacq.) Cogn., leaf extracts on free radicals induced oxidative damage in the biological system, Oxid. Antioxid. Med. Sci. 6 (2017) 14–18.

[48] D.A. Jamdade, D. Rajpali, K.A. Joshi, R. Kitture, A.S. Kulkarni, V.S. Shinde, J. Bellare, K.R. Babiya, S. Ghosh, *Gnidia glauca*- and *Plumbago zeylanica*-mediated synthesis of novel copper nanoparticles as promising antidiabetic agents, Adv. Pharmacol. Sci. 2019 (2019).

[49] G. Das, J.K. Patra, T. Debnath, A. Ansari, H.-S. Shin, Investigation of antioxidant, antibacterial, antidiabetic, and cytotoxicity potential of silver nanoparticles synthesized using the outer peel extract of *Ananas comosus* (L.), PloS One 14 (2019), e0220950.

[50] M. Govindappa, B. Hemashekhar, M.-K. Arthikala, V.R. Rai, Y.L. Ramachandra, Characterization, antibacterial, antioxidant, antidiabetic, anti-inflammatory and antityrosinase activity of green synthesized silver nanoparticles using *Calophyllum tomentosum* leaves extract, Results Phys 9 (2018) 400–408.

[51] V. Malapermal, I. Botha, S.B.N. Krishna, J.N. Mbatha, Enhancing antidiabetic and antimicrobial performance of *Ocimum basilicum* and *Ocimum sanctum* (L.) using silver nanoparticles, Saudi J. Biol. Sci. 24 (2017) 1294–1305.

[52] A. Lateef, M.A. Azeez, T.B. Asafa, T.A. Yekeen, A. Akinboro, I.C. Oladipo, L. Azeez, S.A. Ojo, E.B. Gueguim-Kana, L.S. Beukes, Cocoa pod husk extract-mediated biosynthesis of silver nanparticles: its antimicrobial, antioxidant and larvicidal activities, J. Nanostructure Chem. 6 (2016) 159–169.

[53] J.A. Elegbede, A. Lateef, M.A. Azeez, T.B. Asafa, T.A. Yekeen, I.C. Oladipo, A.S. Hakeem, L.S. Beukes, E.B. Gueguim-Kana, Silver-gold alloy nanoparticles biofabricated by fungal xylanases exhibited potent biomedical and catalytic activities, Biotechnol. Prog. 35 (2019) e2829.

[54] A. Hussain, M.F. Alajmi, M.A. Khan, S.A. Pervez, F. Ahmed, S. Amir, F.M. Husain, M.S. Khan, G.M. Shaik, I. Hassan, R.A. Khan, Md-T Rehman, Biosynthesized silver nanoparticle (AgNP) from *Pandanus odorifer* leaf extract exhibits anti-metastasis and anti-biofilm potentials, Front. Microbiol. 10 (2019).

[55] M. Akter, Md-T. Sikder, Md-M. Rahman, A.K.M.A. Ullah, K.F.B. Hossain, S. Banik, T. Hosokawa, T. Saito, M. Kurasaki, A systematic review on silver nanoparticles-induced cytotoxicity: physicochemical properties and perspectives, J. Adv. Res. 9 (2018) 1–16.